JOURNAL OF IRON AND STEEL RESEARCH, INTERNATIONAL. 2016, 23(6): 593-601

Effects of TMCP Schedule on Precipitation, Microstructure and Properties of Ti-microalloyed High Strength Steel

Xiang-dong HUO[1], Lie-jun LI[2], Zheng-wu PENG[2], Song-jun CHEN[1]
(1. School of Material Science and Engineering, Jiangsu University, Zhenjiang 212013, Jiangsu, China; 2. School of Mechanical and Automotive Engineering, South China University of Technology, Guangzhou 510641, Guangdong, China)

Abstract: Using the similar compositions of the Ti-microalloyed high-strength steels produced by the thin-slab casting process of compact strip production (CSP), four thermo-mechanical control processes (TMCP) after the simulated thick-slab casting, i. e. the two hot rolling routes and the two cooling processes, were designed, aiming at achieving the same mechanical properties as the thin strip products. The final microstructures after the four TMCP processes were examined by optical microscope (OM), scanning electron microscope (SEM) and transmission electron microscope (TEM). The tensile properties and Charpy impact energy were measured correspondingly. Strain-induced TiC precipitation was found in the two-stage rolling route with the finish rolling temperature at low levels, leading to grain refinement due to the pinning effect during austenite recrystallization. Precipitation hardening in ferrite was observed when a period of isothermal holding was applied after hot rolling. It could be concluded that both finish rolling temperature and the subsequent isothermal holding temperature were crucial for the achieved strength level due to the combined effect of grain refinement and precipitation hardening. At the same time, it was found that the isothermal holding led to poor impact toughness because of remarkable precipitation hardening. Therefore, it was suggested that the precipitation kinetics of titanium carbides in both austenite and ferrite should be investigated in future.

Key words: thermo-mechanical control process; compact strip production; titanium carbide; grain refinement; precipitation hardening; Ti-microalloyed high strength steel

Recently, the hot-rolled steels have been extensively studied to exhibit higher strength level for the further mass reduction of structural steel components in the combination of thermo-mechanical control process (TMCP) and microalloying technologies[1-3]. As an economical and effective microalloying element, titanium has attracted more and more attention in recent years[4-6], because it has a lot of beneficial influences on the microstructural evolution during manufacturing process and the final mechanical properties of steel products. For examples, Ti, just like boron element, sometimes is deliberately added to improve the hot ductility of low-alloyed and Nb-contained microalloyed steels to avoid the surface cracking during continuous casting, because the addition of Ti often induces nuclei of precipitation at high temperature in austenite[7-9]; either addition of Ti alone or together with niobium or molybdenum, makes the hot rolled steels obtain yield strength higher than 700 MPa as already developed[10-13]. Particularly, precipitation of TiC has been intensively investigated during heat treatments such as annealing[14] and tempering[15] even within a strong magnetic field[16]. Recently, the hot rolled steel with yield strength of 700 MPa has been successfully produced via the compact strip production (CSP) process and Ti-microalloying technology[17-20], and the precipitation behavior of TiC and strengthening mechanism have been investigated[18,19].

An excellent structural material demands high strength and superior toughness simultaneously; unfortunately, strength and toughness are generally mutually exclusive. Although the high strength steels have been developed by using Ti-microalloying technology and their strengthening mechanism has been clarified, the mechanism on toughening was scarcely reported. Moreover, most of the studies were actually for the hot rolled strip products which were

Biography: Xiang-dong HUO, Doctor, Associate Professor; **E-mail**: hxdustb@163.com; **Received Date**: June 10, 2015

produced by hot rolling in tandem rolling mill, followed by laminar cooling and coiling. However, the medium and heavy steel plates underwent different cooling routes after the end of laminar cooling. Therefore, the different TMCP processes could be designed and their effects on the microstructures and properties could be systematically investigated.

In this study, the Ti-microalloyed high-strength steels which had the same chemical composition and were all produced in the CSP process line were investigated, but rather different TMCP routes were applied to simulate the medium and heavy plate production. The mechanical properties and microstructure, particularly precipitation behavior, were examined; the effects of different TMCP processes were analyzed; the strengthening-toughening mechanism of Ti-microalloyed steel was discussed.

1 Experimental Materials and Procedures

The hot-rolled Ti-microalloyed high strength steel strip was successfully produced industrially in the CSP process line of Zhujiang Steel Co., Ltd., whose process is shown schematically in Fig. 1. The liquid steel was teemed from the tundish into the thin slab caster, in which it was solidified into a continuous slab with a thickness of 60 mm. After it was cut into a specified length, the stocks of slab were then directly charged into the tunnel furnace and soaked at 1150 ℃ for about 20 min before tandem rolling. Six-stand finishing train was employed to produce such a thin hot rolled strip with the thickness of 4 mm, which then entered the run-out table for the accelerated cooling using sprayed water mist until coiling. The finish rolling temperature and coiling temperature were 880 ℃ and 600 ℃, respectively. Such a steel strip produced in the steel industry was cited in this paper as a reference for comparison.

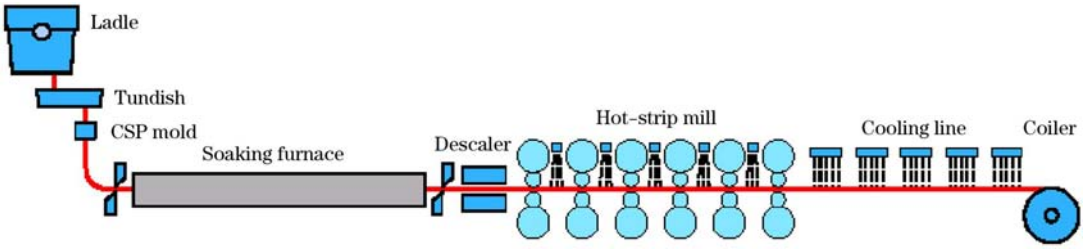

Fig. 1 Schematic diagram of compact strip production process

Besides, a steel was also melted in a vacuum induction furnace, with its compositions being close to those of the reference steel and given in Table 1. The melt was cast into ingot in vacuum, from which two pieces of slabs were cut with dimensions of 150 mm×150 mm×200 mm. They were then hot-rolled to the thickness of 20 mm on a laboratory four-high reversing mill. Four TMCP processes were employed in this study, as detailed below.

Table 1 Chemical compositions of investigated steels mass%

Investigated steel	C	Si	Mn	P	S	Cu	Cr	Ni	Ti	N
Reference steel strip	0.05	0.23	1.10	0.008	0.001	0.25	0.55	0.15	0.12	0.0065
Developed steel plate	0.05	0.27	0.96	0.007	0.003	0.26	0.49	0.19	0.11	0.0032

The slabs were firstly heated to 1200 ℃, held for 90 min for solution treatment and then cooled in air to the start rolling temperature (SRT) of 1150 ℃. The hot rolling process was composed of eleven passes, in which the initial and final thickness is 150 and 20 mm, respectively. Two rolling strategies were adopted by considering the austenitic recrystallization and strain-induced precipitation to different extents: (1) Single-stage rolling schedule. The eleven rolling passes were fully completed in the temperature range of 1150—1030 ℃. (2) Two-stage rolling schedule. The slab was firstly rolled into 75 mm in thickness after five passes at 1150—1030 ℃, then cooled in air to 900 ℃, and further rolled into the thickness of 20 mm in six passes with the finish rolling temperature (FRT) of 850 ℃. Subsequently, the steel plates were cooled with sprayed water at about 20 ℃/s to the final cooling temperature (FCT) of 600 ℃ with two cooling processes. One is that the plate was directly cooled in air (AC) to room temperature. The other is that the plate was put into a muffle furnace for the isothermal holding (IH) at 600 ℃ for 60 min, and then cooled in air to room temperature. The detailed parameters of four differ-

ent TMCP procedures are listed in Table 2.

Specimens for tensile tests were cut from the plates in the longitudinal direction and were tested at room temperature on a Zwick Z450 machine according to the ASTM E 8M-04 standard. Charpy impact tests were performed at the temperature of 20 ℃, 0 ℃, −20 ℃, and −40 ℃, respectively, for sub-size Charpy V-notch (CVN) specimens with size of 5 mm×10 mm×55 mm, which were machined from the middle part of the rolled plates along the transverse direction, and conducted on a Zwick/Roell RKP machine in accordance with the standard method in ASTM E 23-02.

Table 2 Actual rolling and cooling parameters of experimental steels

Steel		TMCP code	SRT/℃	FRT/℃	FCT/℃	Subsequent route
Reference steel		TR	1150	880	600	Tandem rolling and coiling at 600 ℃
Developed steel plate	A	1S-AC	1139	1014	581	Single-stage rolling followed by air cooling
	B	1S-IH	1139	1014	581	Single-stage rolling followed by isothermal holding
	C	2S-AC	1152	852	585	Two-stage rolling followed by air cooling
	D	2S-IH	1152	852	585	Two-stage rolling followed by isothermal holding

Metallographic specimens were cut from plate parallel to the rolling direction. They were ground, polished and finally etched with 3 vol. % nital before they were observed under a LEICA DM 2500M optical microscope (OM) and a JSM-7001F field emission scanning electron microscope (SEM). Thin foils were also prepared from the specimens. They were electropolished on a twin-jet polisher, using a solution of 90 vol. % ethanol and 10 vol. % perchloric acid before they were examined using a JEM-2100 transmission electron microscope (TEM) operated at 200 kV.

2 Results

2.1 Mechanical properties

The mechanical properties of experimental steels are given in Table 3. The reference steel and Plate D exhibit almost the same tensile properties with the yield strength both more than 700 MPa, and have the similar TMCP parameters as shown in Table 2. The strength of produced plates decreases with the sequence of D, B, C and A. The difference in yield strength of Plates A and D exceeds 250 MPa, suggesting that the TMCP parameters significantly influence the mechanical property of developed steels. The yield strengths of Plates B and C are 644.3 MPa and 508.3 MPa, respectively. It can be confirmed that subsequent cooling routes have significant effects on the strength of experimental steels in comparison of Plates A and B or C and D.

Table 3 gives the data of CVN absorbed energy. It can be seen that Plate C has much higher impact energy at the temperature from −40 ℃ to 20 ℃ than Plates D, A and B. The single-stage rolling schedule with high finish rolling temperature (1014 ℃) obviously results in worse toughness. Moreover, under the same rolling condition, isothermal aging at 600 ℃ leads to decreased CVN absorbed energy at the same temperature. The absorbed energy of the reference steel at −20 ℃ is 15.7 J, while that of Plate D is 11.7 J.

Table 3 Mechanical properties of developed steel plates and reference steel

Steel	Yield strength/MPa	Tensile strength/MPa	Yield ratio	Elongation/%	Absorbed energy/J			
					20 ℃	0 ℃	−20 ℃	−40 ℃
Reference steel	730.0	805.0	0.91	26.0	15.7			
Plate A	461.3	697.7	0.66	20.2	8.7	7.0	5.7	4.0
Plate B	644.3	791.3	0.81	21.8	3.7	4.0	3.0	2.7
Plate C	508.3	730.0	0.70	23.3	175.7	98.3	50.7	34.1
Plate D	719.7	808.0	0.89	23.5	28.4	21.7	11.7	4.9

2.2 Microstructure

Fig. 2 shows the optical micrograph at the mid-thickness of the reference steel. Its microstructure is composed of quasi-polygonal ferrite grains, in which some grains elongate along the rolling direction. Electron backscattered diffraction (EBSD) was used to determine the micro-texture of reference steel with a step of 0.5 μm. Fig. 3 shows EBSD orientation maps and frequency distributions of ferrite grain boundary misorientation. Intercept method was used for the grain size measurement and the average size of grains with high angle boundaries (>15°) is 3.3 μm, which

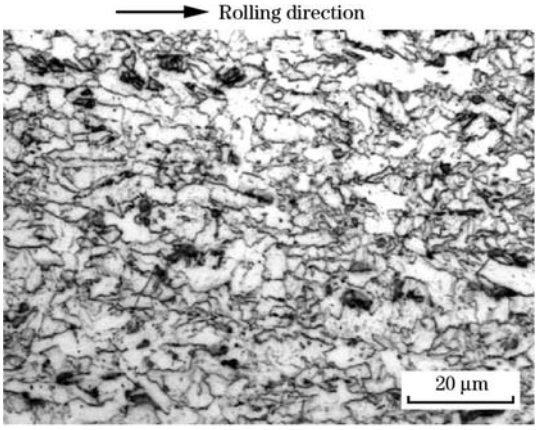

Fig. 2 Optical micrograph of the reference steel

is considered as the valid grain size of Hall-Petch equation. The percentage of high angle boundaries is 56.4%.

Optical micrographs of the developed steel plates are presented in Fig. 4. It can be seen that the microstructures are significantly influenced by the different rolling schedules. Two-stage rolling with low finish rolling temperature of 852 ℃ (Plates C and D) dramatically leads to grain refinement compared to single-stage rolling at high rolling temperature (Plates A and B). The microstructures of Plates A and B are composed of granular bainite and polygonal ferrite; however, the primary microstructural constituent of Plates C and D is mainly quasi-polygo-

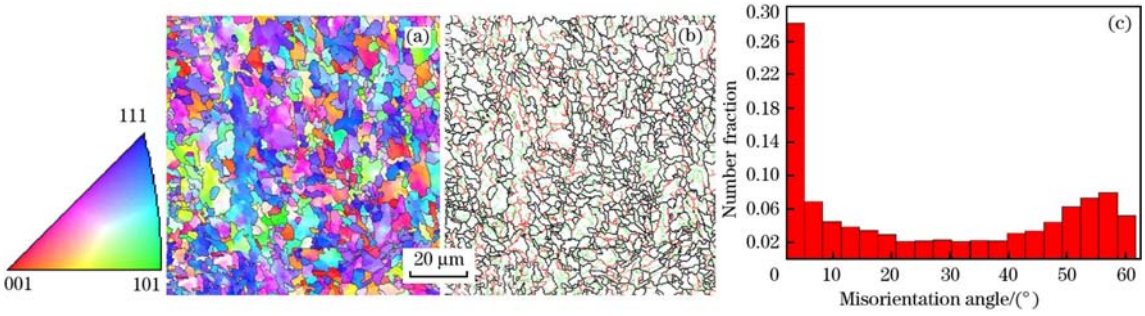

Fig. 3 EBSD orientation maps of the reference steel (a, b) and frequency distributions of ferrite grain boundary misorientation (c)

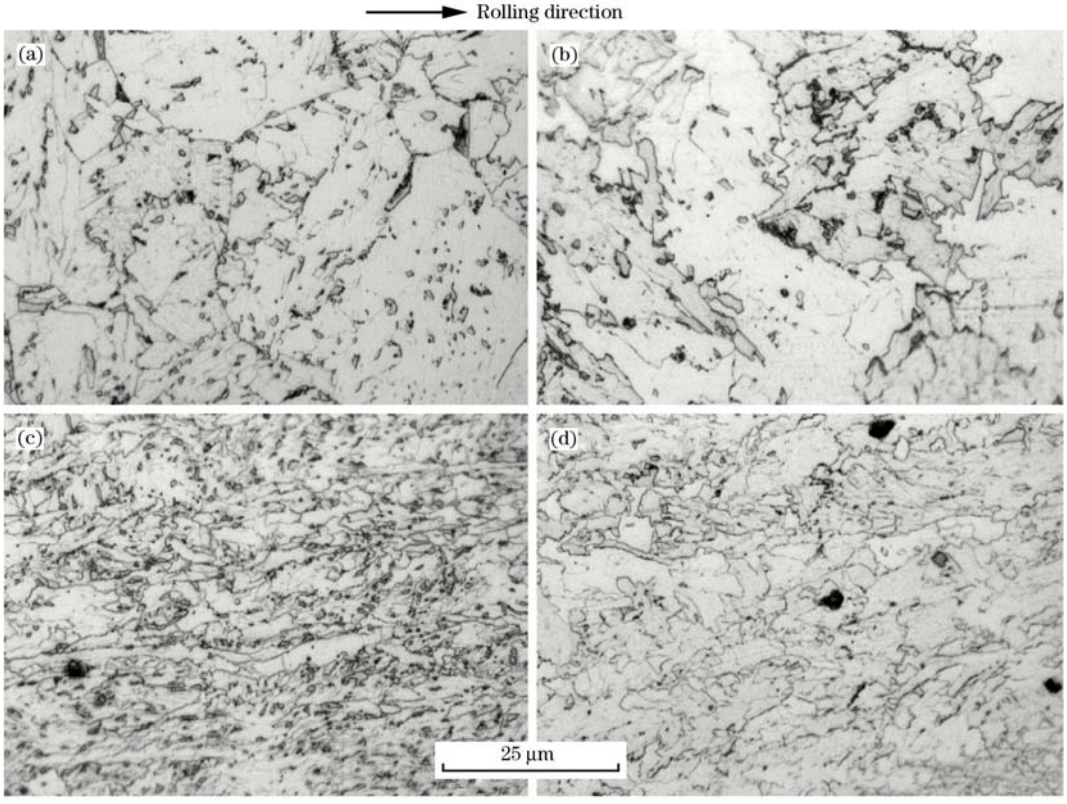

(a) Plate A; (b) Plate B; (c) Plate C; (d) Plate D.

Fig. 4 Optical micrographs of developed steel plates subjected to different TMCP schedules

nal ferrite grains. It is noted that the further cooling mode after laminar water-cooling has little influence on microstructures. Isothermal holding at 600 ℃ just slightly leads to grain growth in comparison with the direct air-cooling, and the primary microstructural constituents in Fig. 4 are similar. SEM micrographs of experimental steels are shown in Fig. 5. The size of martensite/austenite (M/A) constituent is several microns in the case of single-stage rolling, whereas, its size is much smaller in Plates C and D that are subjected to the two-stage rolling. Under the same rolling condition, isothermal holding obviously leads to the decrease in number and size of M/A islands in comparison with the direct air cooling.

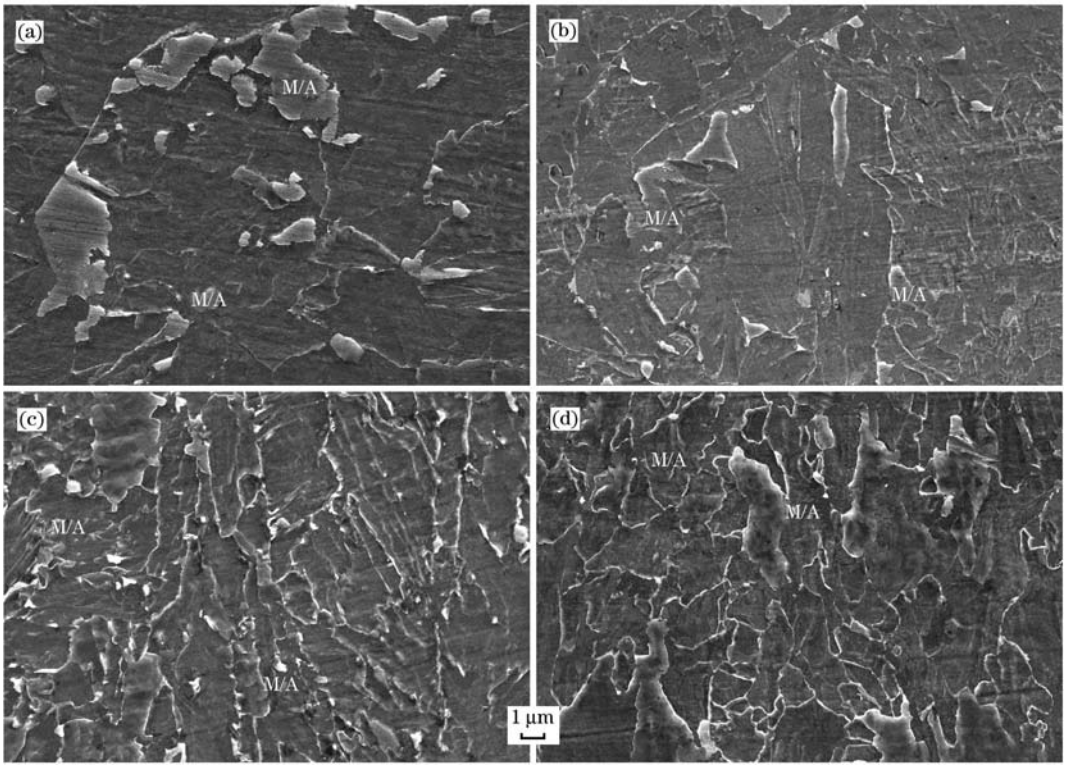

(a) Plate A; (b) Plate B; (c) Plate C; (d) Plate D.

Fig. 5 SEM images of developed steel plates subjected to different TMCP schedules

2.3 Precipitates

TEM micrographs shown in Fig. 6 clearly exhibit a cell-like distribution of several tens nanometer particles in Plates C and D subjected to two-stage rolling with lower finish rolling temperature (852 ℃), implying that the precipitates nucleated on dislocations or on dislocation sub-structures. However, this kind of particles can hardly be observed in steel

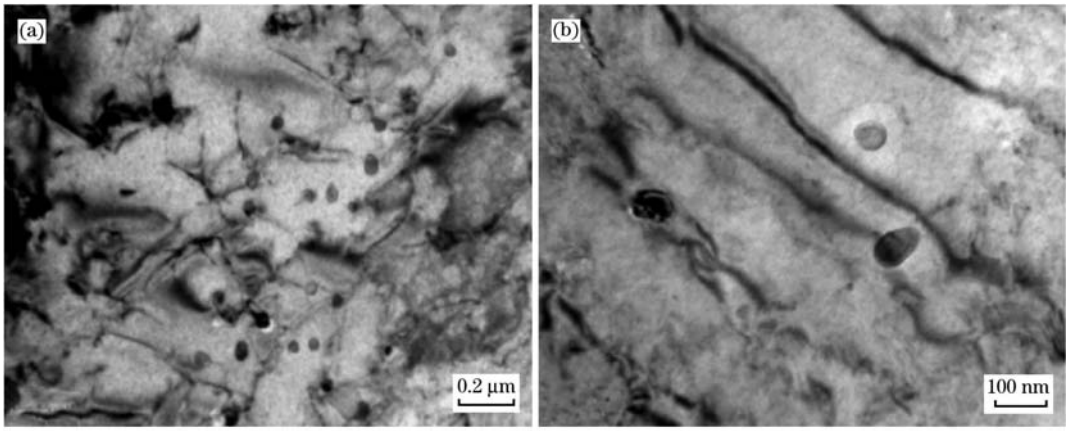

Fig. 6 TEM micrographs of particles in plate subjected to lower finish rolling temperature

plate subjected to single-stage rolling at high temperature.

Fig. 7 shows transmission electron micrographs of developed steel plates. It can be seen that under the same rolling condition, large amount of nanometer particles exist in the steel plate subjected to isothermal aging at 600 ℃. However, this kind of particles are fewer in the specimen air-cooled directly to room temperature.

Representative TEM micrograph of nanometer precipitates in the reference steel is given in Fig. 8. Electrolytically extracted phase analysis shows that the

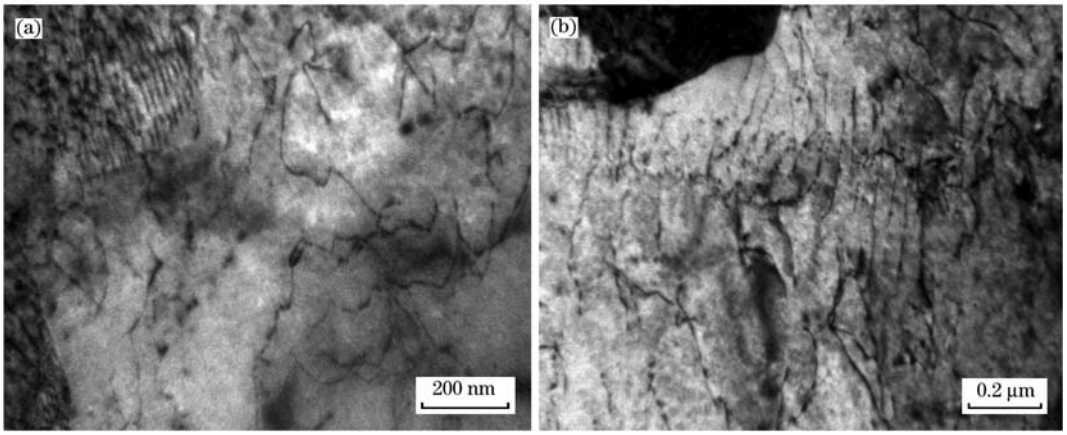

(a) Plate C, direct air cooling; (b) Plate D, isothermal aging at 600 ℃ for 60 min.

Fig. 7 TEM micrographs of developed steel plates

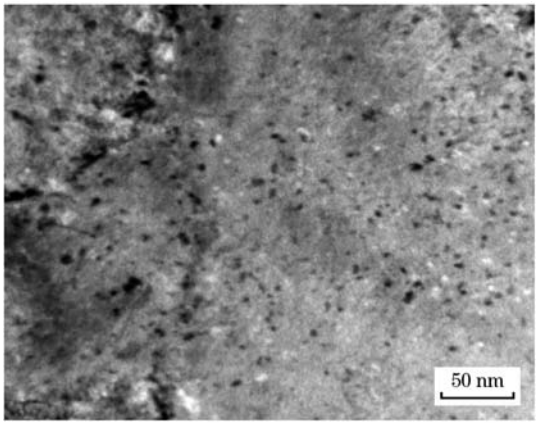

Fig. 8 TEM micrograph of nanometer particles in reference steel

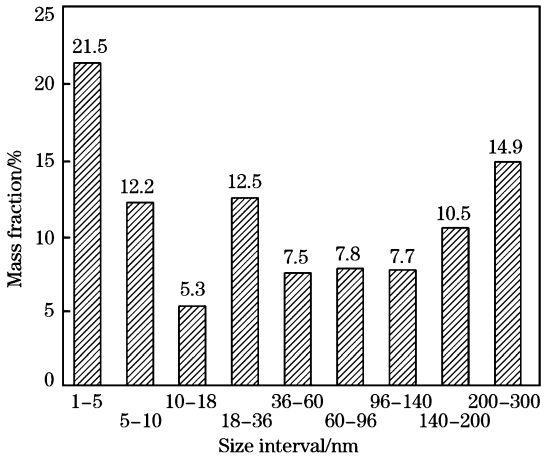

Fig. 9 Size distribution of MX phase in the reference steel

total amount of precipitation phase MX (M=Ti, Mo, Cr; X=C, N) in the reference steel is 0.0793 mass%. The particles of MX are in the size range of 1—300 nm, as measured by the X-ray small angle scattering method. The size distribution of these particles is shown in Fig. 9. The mass fraction of particles smaller than 10 nm accounts for 33.7% of the total MX precipitates.

3 Discussion

3.1 Titanium carbides

Titanium exhibits a strong tendency to form oxides and sulfides as well as nitrides and carbides in steel. The solubility product of titanium compounds indicates that the precipitation sequence of them in steel is $Ti_2O_3 \rightarrow TiN \rightarrow Ti_4C_2S_2 \rightarrow TiC$ with decreasing temperature. The developed steel was melted in a vacuum induction furnace, and the contents of oxygen and sulfur were very low. TiN precipitates at higher temperature; thus, only titanium carbides are discussed as follows. The solubility products of TiC in austenite and ferrite can be expressed as follows[21].

$$\log(w_{[Ti]}w_{[C]})_\gamma = -7000/T + 2.75 \quad (1)$$

$$\log(w_{[Ti]}w_{[C]})_\alpha = -9575/T + 4.40 \quad (2)$$

The contents of titanium, nitrogen and carbon in the developed steel are 0.11 mass%, 0.0032 mass% and 0.05 mass%, respectively. Amount of Ti available

for TiC formation was calculated as $w_{[Ti]}=0.11-(48/14)\times0.0032=0.099$. The solution temperature (T) of TiC in developed steel was calculated as 1112 ℃. The slabs were reheated at 1200 ℃ for 90 min before hot rolling. Therefore, TiC can be fully dissolved in developed steel before hot rolling.

According to Eq. (1), the theoretical precipitation temperature of TiC in the developed steel is 1112 ℃, but the actual precipitation behavior depends primarily on precipitation kinetics. Wang et al.[22] investigated a 0.05% C-0.10% Ti (mass%) high-strength low-alloy (HSLA) steel, having similar composition with the developed steel, and found that the precipitation of TiC did not occur at 975 ℃ and the nucleation of strain-induced TiC precipitation was a very rapid process in the temperature range of 900 — 925 ℃. Obviously, titanium carbides in Plates A and B can hardly precipitate at the finish rolling temperature of 1014 ℃. Thus, grain refinement could only be achieved through austenite recrystallization during the rolling passes in Plates A and B; however, higher temperature allows the growth of recrystallized austenite grains between different passes, weakening the grain refinement effect. On the other hand, strain-induced TiC precipitation took place at low temperature during the second rolling stage in Plates C and D. The fine particles effectively retard recovery and recrystallization of deformed austenite, thus help to retain the accumulated strain and deformed structures of austenite grains, consequently leading to an increase of nucleation sites for $\gamma\rightarrow\alpha$ phase transformation and favoring the refinement of the finial microstructure. For this reason, grain size of Plates C and D subjected to two-stage rolling was remarkably reduced as compared to those of Plates A and B whose finish rolling temperature was 1014 ℃. This gives a reasonable explanation for the grain refinement of Plates C and D shown in Figs. 4 and 5 and for the strain-induced precipitation shown in Fig. 6. Therefore, strain-induced TiC precipitation plays an important role in influencing microstructural evolution during the hot rolling of Ti-microalloyed steel plate. However, precipitates formed in austenite are subjected to a relatively fast coarsening and lose coherency with austenite during transformation to ferrite, so their hardening effect can be ignored.

Mao et al.[23] investigated the 0.5Mn-0.112Ti (mass%) steel and found that its start and finish transformation temperatures at the cooling rate of 20 ℃/s were 800 ℃ and 600 ℃, respectively. As similar composition and cooling rate were adopted in the experimental steel, it can be concluded that $\gamma\rightarrow\alpha$ transformation has been completed during water cooling after hot rolling. According to Eqs. (1) and (2), the equilibrium solubility of TiC in austenite at 852 ℃ is 3.37×10^{-4} and that in ferrite at 600 ℃ is 2.70×10^{-7}. After hot rolling, rapid cooling of experimental steels on run-out table will inhibit the precipitation of titanium carbides and lead to a high degree of supersaturation in ferrite matrix. Isothermal holding at 600 ℃ can promote TiC fully precipitating from supersaturated ferrite solid solutions because the equilibrium solubility at this temperature is extremely low. However, air cooling directly leads to a high degree of supersaturation in ferrite matrix; thus, nanometer particles can hardly be observed in Plates A and C.

It can be confirmed that the cooling route after water cooling becomes the crucial stage for TiC precipitation in Ti-microalloyed steel. Solubility gap of TiC in different phases promotes γ/α interface precipitation during transformation, or titanium carbides may nucleate in supersaturated ferrite. It is noted that different cooling routes after water cooling are adopted for strip production or medium and heavy plate production. In present work, the option of isothermal holding was based on coiling process of strip production, and direct air cooling simulated the cooling route after water cooling during medium and heavy plate production. It is obvious that isothermal holding is beneficial for TiC precipitation in comparison with direct air cooling. Too low coiling temperature will lead to insufficient precipitation, but too high coiling temperature can coarsen the precipitates and lower their strengthening potential. Carbide precipitation under the condition of continuous cooling was investigated and more carbide can precipitate from the supersaturated solid-solution ferrite at the relatively slow cooling rates[24]. Thus, direct air cooling is not beneficial to TiC precipitation because of relatively high cooling rate. Wang et al.[25] found that the precipitation kinetics of nano-size TiC particles in ferrite depended on the annealing temperature, and interface precipitation happened at high temperature such as 700 ℃, 725 ℃, and 750 ℃, but carbides randomly distributed in the ferrite matrix after annealing at 650 ℃ and 675 ℃. This implies that transformation affects TiC precipitation, interface precipitation takes place during $\gamma\rightarrow\alpha$ transformation and dispersed precipitation forms in the ferrite matrix after transformation.

3.2 Strengthening and toughening mechanism

The relationship between yield strength and microstructure can be predicted by the following equation.

$$\sigma=\sigma_0+\sigma_s+\sigma_g+\sigma_p+\sigma_d \quad (3)$$

where, σ_0 is the lattice friction stress with the value of 48 MPa; and σ_s, σ_g, σ_p, and σ_d are the strengthening effects caused by solid solution, grain refinement, precipitation and dislocation, respectively.

Grain refinement hardening effect can be calculated by the well-known Hall-Petch equation

$$\sigma_g=k_y d^{-1/2} \quad (4)$$

where, d is the average ferrite grain size; k_y is constant and its value is 0.55 MPa·$m^{1/2}$ (17.4 N/$mm^{3/2}$) for HSLA steels. The calculation results show that grain refinement effect for the reference steel is 303 MPa.

The well-known Ashby-Orowan model is widely used to calculate the precipitation hardening effect[26].

$$\sigma_p(\text{MPa})=\frac{5.9\sqrt{f}}{\bar{x}}\cdot\ln\left(\frac{\bar{x}}{2.5\times10^{-4}}\right) \quad (5)$$

where, f is the volume fraction of precipitates; and $\bar{x}$ is the mean diameter of particles in micron. Calculating from the results of electrolytically extracted phase analysis for the reference steel, the precipitation hardening effect of nanometer TiC particles is about 158 MPa.

The results revealed that the reference steel is strengthened mostly by combined effects of grain refinement and precipitation hardening. Although dislocation hardening and solid solution hardening cannot be overlooked, the difference between developed steel plates is smaller when the conventional TMCP parameters are adopted for the same compositions. Therefore, the strengthening mechanism of developed steel plates is discussed on the basis of grain refinement and precipitation hardening.

It can be concluded from the previous discussion that lower finish rolling temperature (852 ℃) leads to finer grain size, and isothermal holding at 600 ℃ promotes the precipitation of nanometer TiC. Plate D underwent the similar TMCP parameters as the reference steel, so its yield strength exceeds 700 MPa because of remarkable grain refinement and remarkable precipitation hardening. The yield strength of Plate A is the smallest because of high finish rolling temperature (1014 ℃) and air-cooling directly after water cooling. Strength of other steel plates lies between them. Table 4 shows the strengthening and toughening mechanism of developed steel plates. The values in parentheses are the difference between the properties of Plate A and other plates.

It is well known that grain refinement is the only method to simultaneously improve both strength and toughness. However, precipitation hardening severely impairs the impact toughness of structural materials. It can be clearly seen from Table 4 that Plate B demonstrates the worst toughness because of weaker grain refinement and remarkable precipitation hardening, but Plate C boasts the best toughness because of remarkable grain refinement and few precipitates. Although yield strength of reference steel and Plate D exceeds 700 MPa through grain refinement and precipitation hardening, unfortunately, the impact toughness of them is unsatisfactory, mainly due to the precipitation hardening of TiC particles.

Table 4 Effects of grain refinement and precipitation on strength and toughness

Item	Reference steel	Plate D	Plate C	Plate B	Plate A
Grain refinement	Remarkable	Remarkable	Remarkable	No	No
Precipitation hardening	Remarkable	Remarkable	No	Remarkable	No
Yield strength/MPa	730 (268.7)	719.7 (258.4)	508.3 (47)	644.3 (183)	461.3
Absorbed energy at −20 ℃/J	15.7 (10)	11.7 (6)	50.7 (45)	3.0 (−2.7)	5.7

Titanium carbides maybe nucleate in austenite during hot rolling, at the γ/α interface during transformation, or in supersaturated ferrite. Strain-induced precipitation plays an important role in grain refinement. Interface precipitation and dispersed precipitation in ferrite are the main sources for precipitation hardening. It is noted that strain-induced precipitation during hot rolling would adversely affect the precipitation hardening effect by reducing the amount of titanium and carbon in solution. TMCP conditions should be controlled to favor either strain-induced precipitation in austenite or precipitation in ferrite, in order to obtain better strength and impact properties simultaneously. Previous researches on precipitation behavior and precipitation kinetics of titanium carbides were only focused on either strain-induced precipitation[27,28] or interface precipitation and dispersed precipitation in ferrite[29,30]. The relationship between the two kinds of precipitation and the effects of titanium

carbides on strength and toughness were scarcely reported either. In order to obtain a better strength and impact properties, more TMCP schedules should be extensively investigated in future.

4 Conclusions

(1) Grain refinement was achieved in Plates C and D, which were subjected to lower finish rolling temperature (852 ℃), because strain-induced precipitation inhibited recovery and recrystallization of deformed austenite. Isothermal holding at 600 ℃ promoted the precipitation of nanometer TiC in Plates B and D; however, supersaturated titanium and carbon had no enough time to precipitate in the directly air-cooled Plates A and C.

(2) The yield strength of Plate D, which adopted the similar TMCP parameters as the reference steel, exceeded 700 MPa. Plate A, which was rolled at high finish rolling temperature (1014 ℃) and air cooled directly after water cooling, showed the minimum yield strength. Plate B showed superior toughness to others because of remarkable grain refinement and weaker precipitation hardening.

(3) Ti-microalloyed steel is strengthened mostly by the combined effects of grain refinement and precipitation hardening. Unfortunately, the latter obviously impairs the impact toughness.

References:

[1] S. Shanmugam, N. K. Ramisetti, R. D. K. Misra, J. Hartmann, S. G. Jansto, Mater. Sci. Eng. A 478 (2008) 26-37.

[2] A. A. Barani, F. Li, P. Romano, D. Ponge, D. Raabe, Mater. Sci. Eng. A 463 (2007) 138-146.

[3] G. W. Yang, X. J. Sun, Z. D. Li, X. X. Li, Q. L. Yong, Mater. Des. 50 (2013) 102-107.

[4] Y. L. Kang, Q. H. Han, X. M. Zhao, M. H. Cai, Mater. Des. 44 (2013) 331-339.

[5] G. Xu, X. L. Gan, G. J. Ma, F. Luo, H. Zhou, Mater. Des. 31 (2010) 2891-2896.

[6] X. D. Huo, X. P. Mao, S. X. Lv, J. Iron Steel Res. Int. 20 (2013) No. 9, 105-110.

[7] H. W. Luo, L. P. Karjalainen, D. A. Porter, ISIJ Int. 42 (2002) 273-282.

[8] H. W. Luo, P. Zhao, Mater. Sci. Technol. 17 (2001) 1589-1595.

[9] H. W. Luo, P. Zhao, Y. Zhang, Mater. Sci. Technol. 17 (2001) 843-846.

[10] H. L. Yi, L. X. Du, G. D. Wang, X. H. Liu, ISIJ Int. 46 (2006) 754-758.

[11] N. Nakata, M. Militzer, ISIJ Int. 45 (2005) 82-90.

[12] R. D. K. Misra, H. Nathani, J. E. Hartmann, F. Siciliano, Mater. Sci. Eng. A 394 (2005) 339-352.

[13] Z. Q. Wang, X. J. Sun, Z. G. Yang, C. Zhang, Mater. Sci. Eng. A 573 (2013) 84-91.

[14] Z. X. Xia, C. Zhang, Z. G. Yang, Mater. Sci. Eng. A 528 (2011) 6764-6768.

[15] T. Peng, C. Zhang, Z. G. Yang, J. Iron Steel Res. Int. 17 (2010) No. 5, 74-78.

[16] Z. X. Xia, C. Zhang, H. Lan, Mater. Lett. 65 (2011) 937-939.

[17] Y. Funakawa, T. Shiozaki, K. Tomita, T. Yamamoto, E. Maeda, ISIJ Int. 44 (2004) 1945-1951.

[18] X. P. Mao, X. D. Huo, X. J. Sun, Y. Z. Chai, J. Mater. Process. Technol. 210 (2010) 1660-1666.

[19] X. P. Mao, X. J. Sun, Y. L. Kang, Z. Y. Lin, Acta Metall. Sin. 42 (2006) 1091-1095.

[20] C. J. Wang, Q. L. Yong, X. J. Sun, X. P. Mao, Z. D, Li, Acta Metall. Sin. 47 (2011) 1541-1549.

[21] K. A. Taylo, Scr. Metall. Mater. 32 (1995) 7-12.

[22] Z. Q. Wang, X. P. Mao, Z. G. Yang, X. J. Sun, Q. L. Yong, Z. D. Li, Y. Q. Weng, Mater. Sci. Eng. A. 529 (2011) 459-467.

[23] X. P. Mao, Q. L. Chen, X. J. Sun, J. Iron Steel Res. Int. 21 (2014) No. 1, 30-40.

[24] C. Y. Chen, H. W. Yen, F. H. Kao, W. C. Li, C. Y. Huang, J. R. Yang, Mater. Sci. Eng. A 499 (2009) 162-166.

[25] T. P. Wang, F. H. Kao, S. H. Wang, J. R. Yang, C. Y. Huang, H. R. Chen, Mater. Lett. 65 (2011) 396-399.

[26] T. Gladman, D. Dulieu, I. D. Mcivor, in: Proc. of Symp (Eds), On Microalloying 75, Union Carbide Co., New York, 1976. pp. 32-55.

[27] W. K. Yong, S. W. Song, S. J. Seo, S. G. Hong, S. L. Chong, Mater. Sci. Eng. A 565 (2013) 430-438.

[28] Z. Q. Wang, X. J. Sun, Z. G. Yang, Q. L. Yong, C. Zhang, Z. D. Li, Y. Q. Weng, Mater. Sci. Eng. A 573 (2013) 84-91.

[29] Z. Jia, R. D. K. Misra, R. O. Malley, S. J. Jansto, Mater. Sci. Eng. A 528 (2011) 7077-7083.

[30] H. W. Yen, P. Y. Chen, C. Y. Huang, J. R. Yang, Acta Mater. 59 (2011) 6264-6274.